Elsevier Editorial System(tm) for Sensors & Actuators: B. Chemical

Manuscript Draft

Manuscript Number:

Title: Augmented Droplet Actuation and Spreading using Triangular Coplanar Electrodes

Article Type: Research Paper

Keywords: Electrowetting on dielectric (EWOD); electrode geometry; contact line motion; transfer time.

Corresponding Author: Professor Sunando DasGupta, PhD

Corresponding Author's Institution: Indian Institute of Technology Kharagpur

First Author: Mainak Basu

Order of Authors: Mainak Basu; Vedant P Joshi; Soumen Das, PhD; Sunando DasGupta, PhD

Abstract: The geometry of the coplanar electrodes during electrowetting on dielectric (EWOD) plays a crucial role in the dynamics of droplet actuation and motion and the resulting phenomena are important in a number of applications. Herein, a strategically placed array of triangular electrodes resulted in a zigzag motion of the droplet. Because of the shape and orientation of the electrodes, the effective contact line moves in different directions after every switching. The displacements, velocities and transfer times are measured to characterize droplet motion. A force balance involving the effects of electrocapillary (driving force) and the resistive forces, such as the hydrodynamic force and the contact line friction force is developed to probe the physics of droplet dynamics on such platforms. The transfer time and the average droplet velocities on triangular electrodes are compared with those on conventional square electrodes. Further, the spreading dynamics of droplet actuation is probed to elucidate its unique characteristics including the enhancement of transport rate for the specific electrode geometry. The resulting insights will be helpful in a number of lab-on-chip applications.

Suggested Reviewers: Joel Plawsky Sc.D.,PhD,MS,BS
Professor, Howard P. Isermann department of Chemical and Biological Engineering, Rensselaer Polytechnic Institute
plawsky@rpi.edu
Eminent researcher in the field of interfacial phenomenon, transport process, microelectronics.

Justin Weibel Ph.D, B.S.
Research Associate Professor, School of Mechanical Engineering and Brick Nanotechnology Center, Purdue University
jaweibel@purdue.edu
Research area in microscale and nanoscale transport phenomena.

Siddhartha Panda Ph.D, M.S., B.Tech

Professor, Department of Chemical Engineering, Indian Institute of Technology Kanpur
spanda@iitk.ac.in
Research area on microfluidics, microscale transport process, micro and nano fabrications.

Alice Tang Turner Ph.D
Managing editor, Department of Physics, Chemistry and Biology, Sensor and Actuator Systems, Linköping University
alice.tang-turner@liu.se
Managing editor of Elsevier's Biosensors and Bioelectronics journal.

Rahul Roy PhD, B-Tech (Hons.)
Assistant Professor, Department of Chemical Engineering, Indian Institute of Science
rahulroy@iisc.ac.in
Research area on Microfluidics and Bio-microfluidics.

Cover letter

To: The Editor
Journal of Sensor and Actuators B

Date: August 30, 2019

Dear Sir/Madam,

Please find attached a manuscript entitled: 'Droplet Actuation and Spreading on Triangular Coplanar Electrodes' by Mainak Basu, Vedant P. Joshi, Soumen Das, Sunando DasGupta, for consideration as a '**regular article**' in your journal.

The geometry of the coplanar electrodes during electrowetting on dielectric (EWOD) plays a crucial role in the dynamics of droplet actuation and motion. In the present study, a unique design of triangular electrodes on the DMF platform resulted in a zigzag motion of the droplet during electrowetting due to the continuous changing of the direction of the net motive force at the contact line. A model based on a force balance approach between the driving and the resistive forces is developed and the resulting equations are used to analyze the experimental trends and results providing insight into the transport phenomena at the microscale. The droplet spreading dynamics is thoroughly probed with the help of the characteristic time scales (ξ) at the under damped and over damped regimes during spreading. These results and analysis may help in developing micro-actuators with faster response in lab-on-chip applications.

I certify that this manuscript or any part of it, has not been published and will not be submitted elsewhere for publication while being considered by your journal. All authors have read and approved the manuscript.

Thank you very much for your time and consideration. I will be glad to furnish any further details that you may require.

Best regards,

Prof. Sunando DasGupta
Professor of Chemical Engineering, IIT Kharagpur, INDIA.

Augmented Droplet Actuation and Spreading using Triangular Coplanar Electrodes

GRAPHICAL ABSTRACT

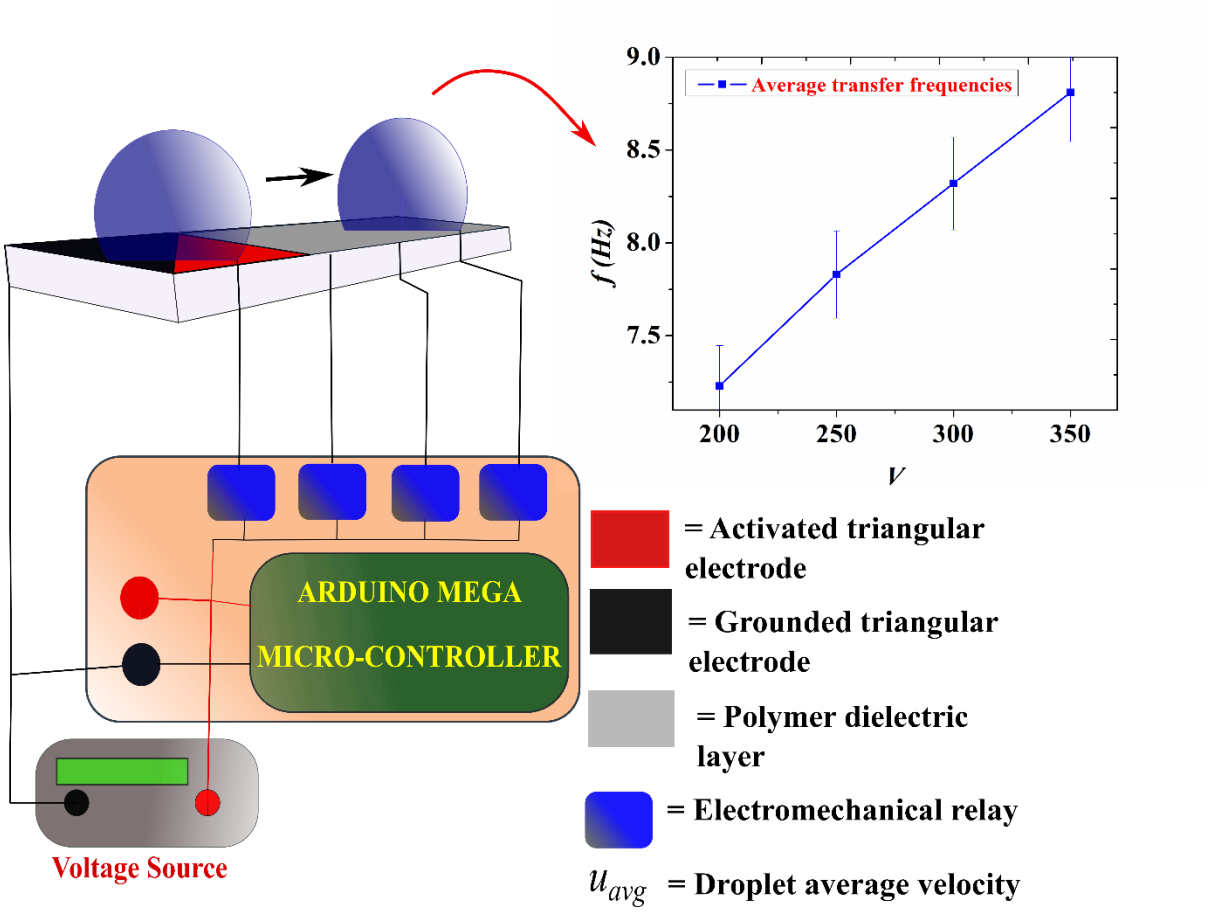

f **= Average Transfer frequencies**

RESEARCH HIGHLIGHTS:

- Equilateral triangular coplanar electrodes are designed and fabricated with a dielectric and a protective hydrophobic layer to study the enhanced dynamics and zigzag motion of the droplets and compared with results from a square electrode array.
- The droplet spreading dynamics is found in the underdamped regime. Furthermore, a transient force balance approach including the effect of contact line friction is adopted to develop expression for the droplet velocity under varying operating conditions and successfully compared with the experimental data.

Augmented Droplet Actuation and Spreading using Triangular Coplanar Electrodes

Mainak Basu[1], Vedant P. Joshi[3], Soumen Das[1, 2], Sunando DasGupta[1, 3, *]

[1]*Advanced Technology Development Centre, Indian Institute of Technology Kharagpur, India*

[2]*School of Medical Science and Technology, Indian Institute of Technology Kharagpur, India*

[3]*Department of Chemical Engineering, Indian Institute of Technology Kharagpur, India*

Abstract

The geometry of the coplanar electrodes during electrowetting on dielectric (EWOD) plays a crucial role in the dynamics of droplet actuation and motion and the resulting phenomena are important in a number of applications. Herein, a strategically placed array of triangular electrodes resulted in a zigzag motion of the droplet. Because of the shape and orientation of the electrodes, the effective contact line moves in different directions after every switching. The displacements, velocities and transfer times are measured to characterize droplet motion. A force balance involving the effects of electrocapillary (driving force) and the resistive forces, such as the hydrodynamic force and the contact line friction force is developed to probe the physics of droplet dynamics on such platforms. The transfer time and the average droplet velocities on triangular electrodes are compared with those on conventional square electrodes. Further, the spreading dynamics of droplet actuation is probed to elucidate its unique characteristics including the enhancement of transport rate for the specific electrode geometry. The resulting insights will be helpful in a number of lab-on-chip applications.

Keywords: Electrowetting on dielectric (EWOD); electrode geometry; contact line motion; transfer time.

[*]Corresponding author, email: sunando@che.iitkgp.ac.in

1. INTRODUCTION

The controlled movement of small discrete droplets on a composite hydrophobic-dielectric film using the principles of electrowetting on dielectric (EWOD) is being used in a number of applications leading to the fast-evolving field of Digital microfluidics (DMF). The transportation of droplet is governed by an applied electric potential in an array of metal electrodes located underneath a dielectric film. There are many applications of DMF e.g., in micro-reactors, in biology such as in low volume biological, biochemical and lab-on-chip operations like enzyme assay[1], point of care devices[2], DNA based applications[3], chemical reactor bed[4]. Other applications include liquid dispensers[4], electronic hotspot cooling[5], electrostatically focused liquid lenses[6], electronic paper display[7], and many others[8-10].

In general, the DMF platform is designed in two configurations: closed and open platform devices[11,12]. In closed DMF devices, droplets are sandwiched between two plates. The bottom electrode acts as the activated electrodes and the top one comprises the ground electrode. This type of configuration is capable to perform, four different microfluidic operations like dispensing, splitting, merging and transporting[10]. On the other hand, single plate open platform configuration[11] is suitable for droplet transportation and works better in merging & mixing, but lack in performing droplet splitting and dispensing[12].

In an open DMF platform, a sessile conductive droplet over the dielectric film covers two adjacent coplanar electrodes. Electrostatic actuation is provided by the application of an electric potential to one of the electrodes while keeping the other grounded. This leads to a reduction in the interfacial energy of the activated electrode, due to the modulation of dielectric charges by applied electric field[12]. This reduction in interfacial energy gives rise to a change in the contact angle over the electrically activated electrode, while the contact

angle remains unchanged over the grounded electrode. This difference between the contact angle of the two parts of a droplet may set forth motion of the droplet[13]. From an experimental perspective, due to the presence of surface micro defects and surface pinning, it requires a minimum actuation voltage (threshold voltage) for droplet actuation[14].

Conventionally DMF platforms are designed with square coplanar electrodes for droplet actuation[15]. It has been pointed out that DMF performance largely depends on the geometry of the coplanar electrodes[16,17]. To achieve smooth transport of droplets with enhanced velocity, various research groups have tried different types of driving electrodes like jagged, crescent, twin plate[18,14], etc. Among them,interdigitated jagged coplanar electrodes turned out to be the best in different lab-on-chip operations[19]. The jagged electrodes perform well for smooth droplet merging and splitting, while crescent electrodes report higher droplet velocity, thus increasing the transport frequency for the DMF device.

In the present study, a new fabrication strategy is presented by strategically placing an array of triangular coplanar electrodes which results in two-directional zigzag motions of the droplets with possible benefits in mixing applications. The instantaneous velocities, acceleration, and average transfer frequencies over the triangular electrodes are measured. A theoretical model based on a force balance approach has been developed taking into account the pertinent forces for droplet motion and to analyze the experimental data to elicit important information on the role of electrode geometry and effect of contact line dynamics.

2. EXPERIMENTATION AND METHODS

The experiments involve actuating the motion of a sessile, conductive liquid droplet over the fabricated triangular coplanar electrode array in an open EWOD mode. A single array consisting of nine identical electrodes having equilateral triangular geometry with a length of each side is equal to 1.5 mm is designed. Each electrode is rotated by an angle of

180˚ with respect to its two neighbors, placed at a uniform gap of 60μm (Fig. 1). The triangular electrodes are covered with a thin layer of PDMS as the dielectric and a thin coating of Teflon as the protective hydrophobic layer. The details of design and fabrication steps are provided in the Supplementary document (Fig. **S1**, Fig. **S2** of section **I and II**).

2.1 EWOD experiments

The sequential activation of the electrode array for droplet actuation and movement is achieved by connecting the fabricated DMF platform to an electronic switching circuit board and power supply along with a high-speed camera (Fig. 2). The board consists of Arduino Mega with ATMEGA as a microcontroller and is connected to a power supply module (Keithley instruments 0-1kV) and the DMF platform through electromagnetic relays for sequential activation (Fig. 2(a)). A high-speed camera (IMPEREX: VGA 210 camera) with a macro lens (IMPEREX: IPX-VGA210-L) is used to capture droplet dynamics at 120 fps (Fig. 2(b)).

2.2 The sequence of electrode actuation and droplet movement

Experiments are performed with 4±1μl droplets of 1mM potassium chloride solution prepared with ultrapure distilled water (Millipore India Pvt. Ltd.). Fig. 3(a) and 3(b) represent the schematic top view and photograph of a sequence of droplet motion and the corresponding switching logic. The droplet is manually dispensed to ensure that its footprint partially overlaps two adjacent triangular electrodes (Fig. 3(a,b)-(i)). A voltage (V) is applied to the 2^{nd} electrode through the activation of relay 1 ensuring positive potential to the 2^{nd} electrode. Once the 2^{nd} electrode gets activated, the droplet (4μl) starts to move from its initial position as shown in Fig. 3(a,b)-(ii) at an actuation voltage of around 175 V.

The foot of the droplet after the first actuation rests between the 2nd and the 3rd electrode. A portion of the droplet may go beyond the 2nd electrode as shown in Fig. 3(a,b)-(iii) as the droplet follows the longest diagonal path of the parallelogram formed by the two adjacent triangular electrodes, to reach its final location (between the 2nd and 3rd electrode).

This is followed by activation of the 3rd electrode using the relay 2 such that the droplet starts moving towards the 3rd electrode. Because of the relative orientation of the two consecutive electrodes, the droplet moves in a zigzag path as shown in Fig. 3(a,b) with the arrows representing the motion. The video of the droplet motion is provided as supporting information and analyzed by an open-source image processing software named 'Tracker' at four different actuating voltages of 200V, 250V, 300V, and 350V.

3. RESULTS AND DISCUSSION

Upon application of an electric field, the droplet starts to spread first, followed by movement once a threshold value is reached. The initiation and actuation are addressed separately.

3.1 Droplet spreading dynamics

The Young-Lippmann equation relates the change in the droplet contact angle upon application of an electric field as $\cos\theta_V = \cos\theta_0 + \frac{\varepsilon_0 \cdot \varepsilon_r}{2 \cdot d \cdot \gamma_{LV}} V^2$ where θ_V is the voltage-dependent contact angle, θ_0 is the initial contact angle; ε_0 and ε_r are the relative permittivity of free space and that of the dielectric layer having thickness *d*; γ_{LV} is the liquid-vapor surface tension and *V* the applied voltage. However, the relation provides the equilibrium contact angles but does not address the transient states of the droplet during actuation. It is mentioned in the literature[20]that the transient behavior of a droplet can be categorized into

two regimes, namely underdamped and overdamped. In a physical system, damping is produced by processes that dissipate the energy stored in the system. In the overdamped regime, the foot radius of the droplet monotonically increases and reaches a steady-state, while in the underdamped regime the increase in the foot radius is significantly more and decays in a sinusoidal fashion before reaching its equilibrium value[20].

The electrocapillary driving force (F_a) acting at the vicinity of the three-phase contact line (TPCL) region of a droplet, F_a can be represented by, $F_a = \gamma_{LV} \cdot (\cos\theta_V - \cos\theta_0) = \gamma_{LV} \cdot \eta$ where η is non-dimensional electrowetting number represented as $\eta = \frac{\varepsilon_0 \cdot \varepsilon_r}{2 \cdot d \cdot \gamma_{LV}} V^2$ and γ_{LV} is the liquid-vapor surface tension.

In the overdamped regime, the dominant opposing friction force is the contact line friction force[21]. If τ_{od} is the characteristic time for spreading of the droplet in the overdamped regime, the contact line velocity can be represented as, $u_{ct} \approx \frac{r_e}{\tau_{od}}$, where $r_e = \beta \cdot r'$ is the spreading radius at equilibrium[20] and $r'$is the radius of the equivalent sphere having the same volume as that of the droplet. β can be derived based on the assumption that the droplet retains its spherical cap shape with its volume conserved and expressed as $\beta = \frac{r_e}{r'} = (1-\cos^2\theta_V)^{1/2} \cdot (4 \cdot (1-\cos\theta_V)^{-2} (2+\cos\theta_V)^{-1})^{1/3}$. By balancing the opposing contact line friction force with the electrocapillary driving force, one can write $\tau_{od} = \frac{\zeta \cdot r_e}{\gamma \cdot \eta}$, with ζ being the contact line friction coefficient.

In the underdamped regime, the viscous force is negligible as compared to the opposing inertial force. By balancing the driving force with the inertial force per unit length, it can be shown that the droplet oscillates with a characteristic frequency [22] and can be

represented as $\omega = \left(\frac{\gamma \cdot \eta}{\rho \cdot (r')^3} \right)^{1/2}$. The characteristic time scale to reach maximum deformation can be represented as $\tau_{ud} = \pi \cdot \left(\frac{\rho \cdot (r')^3}{\gamma \cdot \eta} \right)^{1/2}$.

The prevalence of overdamped and underdamped regime can be ascertained by comparing the two time scales. The ratio of the time scales, denoted by ξ and defined as $\xi = \frac{\tau_{od}}{\tau_{ud}}$ will indicate the nature of the system during spreading. Any value of ξ<1 will represent the underdamped regime and vice versa. The ξ values evaluated for the four operating voltages (expresed as electrowetting number η) are presented in table 1. They clearly demonstrate that the droplet spreading is well in the underdamped regime with dominance of inertial over viscous force for the voltage range used herein.

3.2 Droplet actuation dynamics

A transient force balance approach involving the actuating force and the resistive forces is used to evaluate the droplet velocity. The relevant forces are the electrocapillary inspired driving force (F_a) and resistive forces namely, the hydrodynamic shear force (F_h) and the contact line friction force (F_{cl}). The frictional effect due to drag by the filler fluid (air) can be neglected. The values of the Capillary number (Ca), Bond number (Bo), and Weber number (We) for the droplet of volume 4±1µl (footprint radius of the droplet = 0.96mm) at different applied voltages are found to be Ca = 1.99×10^{-5} to 9.50×10^{-4}; Bo = 0.257 and We = 5.26×10^{-5} to1.19×10^{-3}respectively and the droplet can be considered as part of a sphere. The force balance during droplet transport can be written as,

$$m\frac{du}{dt} = F_a - F_h - F_{cl} \quad (1)$$

where, F_a = driving electro-capillary force, F_h = hydrodynamic force, F_{cl} = three-phase contact line friction force.

The two adjacent triangular coplanar electrodes form a parallelogram. Due to the change in interfacial tension upon application of a potential difference, the droplet experiences a net driving capillary force in a direction perpendicular to the shorter diagonal as shown in Fig. 4. The region at the foot of droplet over which this capillary line force acts is known as the three-phase contact line (TPCL) region (Fig. 4(a), the arc DA of the circle), where the droplet, substrate and the surrounding air are in close proximity.

The capillary line force density acting at the TPCL[15,28]can be represented by,

$$f_0 = \gamma_{LV} \cos\theta_0 \tag{1}$$

where γ_{LV} the surface tension; θ_0 and θ_v are the contact angles in absence and presence of an applied potential. Thus, equation (2) can be modified to include the additional effect of the electric field as described by the Young's-Lippmann (Y-L) equation[23] described earlier,

$$f_a = \gamma_{LV} \cdot (\cos\theta_V - \cos\theta_0) = \frac{\varepsilon_0 \cdot \varepsilon_r}{2 \cdot d} V^2 \tag{2}$$

Since the droplet is moving in a zigzag direction, the TPCL is continually changing. Fig. 4(a-c) shows the position of a droplet traveling across two consecutive triangular electrodes (respective axes are defined specifically in the schematic for better understanding).

The x component of the electrocapillary force (f_a) can be represented as $f_{ax} = f_a \cos 30^\circ$ and the y-component as $f_{ay} = f_a \sin 30^\circ$. The net electrocapillary force (F_a) acting along the arc DA is therefore,

$$F_a = \int_{DA} \sqrt{\left(f_{ax}\right)^2 + \left(f_{ay}\right)^2}\, dl = f_a \cdot \int_{DA} n \cdot dl \ . \tag{4}$$

dl is the unit element of the droplet contour line (arc DA of the circle in Fig. 4(a)), *n* is the unit vector normal to the line. Equation (4) can be rewritten as,

$$F_a = f_a \cdot \int_{DA} n \cdot dl = \gamma_{LV} \cdot (\cos\theta_V - \cos\theta_0) \cdot l = \frac{\varepsilon_0 \cdot \varepsilon_r}{2 \cdot d} V^2 \cdot l \,. \tag{5}$$

Here *l* is the effective length of the contact line length which is the projection of the TPCL over the shorter diagonal of the parallelogram formed by the electrodes. The orientation of the triangular electrodes results in changing the direction of the net driving force at every switching and results in zigzag motion of the droplet over the electrode array and the electro-capillary induced driving force can be written[24,31,32]as,

$$F_a = l \cdot \gamma_{LV} \cdot \left(\cos\theta_V - \cos\theta_0\right) = \left(\frac{l \cdot C_{eq}}{2}\right) \cdot [V_{eff}(t)]^2 \tag{6}$$

Here, θ_V is the instantaneous contact angle and θ_0 is the contact angle at zero voltage (110.5°); with $V_{eff}(t) = V_{eff}{}^0(1 - e^{(-t/RC)})$ and $V_{eff}{}^0 = \sqrt{\left(V^2 - V^2{}_{\min}\right)}$; where V_{min} is the threshold voltage for droplet actuation; C_{eq} is the specific capacitance represented by $C_{eq} = \dfrac{\varepsilon_0}{\left(\dfrac{d_p}{\varepsilon_p} + \dfrac{d_t}{\varepsilon_t}\right)}$ and γ_{LV} is the surface tension measured as 70.01 mN.m; ε_0 is the permittivity of free space, ε_p and ε_t are the dielectric constants of PDMS and Teflon respectively, d_p and d_t are the thicknesses of the PDMS and theTeflon layer respectively.

Incorporation of $V_{eff}{}^0$ instead of *V* includes the surface hysteresis effect into the present model[27]. The gradual spreading of the droplet increases its radius of curvature and results

in a reduction of the liquid pressure at TPCL, with a concomitant change in the capillary force at the TPCL resulting in motion.

The hydrodynamic friction force can be expressed as,

$$F_h = \frac{3\mu_f \pi r(t)^2 u(t)}{4h(t)} \tag{7}$$

Here, μ_f represents the viscosity of the liquid, r is the foot radius of the droplet, h represents the height of the droplet during transportation and *u* the velocity. The values of *r* and *h* at different applied voltages are measured and presented in the supporting document table **S1**. The relation between the contact angle and the footprint radius of the droplet at different applied voltage can be written as[28],

$$r(t) = \left[\frac{3\forall \sin^3 \theta_V}{\pi(2 - 3\cos\theta_V + \cos^3 \theta_V)} \right]^{\frac{1}{3}} \tag{8}$$

where $\forall$ is the droplet volume. The height *h* can be expressed as,

$$h(t) = r(t) \cdot \left(\frac{1 - \cos\theta_V}{\sin\theta_V} \right). \tag{9}$$

Dynamic wetting takes place as the droplet starts to move with displacement of the three-phase contact line. Such displacement of the contact line leads to a dissipation of energy at the molecular level and commonly termed as the contact line friction force[35,36,37], denoted here by F_{cl}. The molecular kinetic theory (MKT) expresses the contact line friction force as,

$$F_{cl} = P\zeta u(t) \tag{10}$$

where ζ is the coefficient of contact line friction[26] and P is the perimeter of the droplet. The origin of the parameter ζ is molecular in nature and depends on the nature and interactions of the molecules at the TPCL region and can be represented as [31],

$$\zeta = \frac{k_B T}{k^0 \lambda^3} \tag{11}$$

The evaluation of ζ is not straightforward and is generally measured in situ from the experimental results. Substituting the expressions of these forces in equation (1) the overall governing equation for droplet motion becomes

$$m\frac{du}{dt} = \left(\frac{l \cdot C_{eq}}{2}\right) \cdot [V_{eff}(t)]^2 - \frac{3\mu_f \pi r^2(t) u(t)}{4h(t)} - P\zeta u(t) \tag{12}$$

The average velocity (u_{avg}) can be represented by numerically solving equation (12) and is expressed as.

$$u_{avg}(t) = \frac{\int_0^{t_a} u(t)dt}{t_a} \tag{13}$$

Where, t_a is the time taken by the droplet to reach steady-state as mentioned in Fig. 5(b) and is a function of the applied voltage. Equation (13) can be used to evaluate the average droplet velocity during electrowetting and compared with the experimentally measured average velocity.

3.3 Evaluation of dynamic characteristics during droplet transportation

The droplet transportation characteristics are measured at different operating voltages. The threshold voltage, at which the droplet start to move is the hysteresis induced minimum actuation voltage (V_{min})[30,31]and is found to be 175V for the present experiments. However,

smooth translation starts for an applied voltage of around 200V. The visualization of the droplet motion clearly indicates that the droplet moves in the direction towards the base of the activated electrode, resulting in a zigzag motion (Fig. 3). The advancing edge of the actuated droplet is tracked from the extracted sequential images of the recorded video. While measuring the displacement of the droplet, the coordinate axis is aligned along the direction of motion of the droplet for a single transport thereby taking into account the two-dimensional motion over the DMF platform. The changes in the droplet movement characteristics for different applied voltage are presented in Fig. 5. Initially, the droplet starts to move upon actuation and is marked in Fig. 5(a) as the 'droplet actuation period'. The droplet reaches its peak displacement where no appreciable changes in diameter and velocity are observable before the beginning of the next actuation. This is termed as the 'droplet settling period' in Fig. 5(a). Since the time scales of droplet motion are quite small the dynamic characteristics are reported in Fig. 5 for durations up to 0.3 s. The charging time of the solid-liquid interface (t_c) is found to be very small (0.015 s) in comparison to the switching time, i.e., $t_c << t_s$ [32]. Due to the accumulation of a net charge in the liquid-solid interface, the resulting electrostatic forces will cause spreading near the contact line, resulting in droplet actuation.

The instantaneous droplet velocities (u) are evaluated and presented in Fig. 5(b) at different applied voltages with the maximum velocity increasing with applied voltage. During droplet transport, the electro-capillary force initially dominates over the frictional forces resulting in a peak in droplet velocity. A dynamic equilibrium is eventually reached between the electrocapillary force and the resisting frictional forces to reach a region where the velocity nearly constant with a very small value and is referred to as the 'droplet settling velocity (v_s)'.

The average transfer frequency (*f*) is the rate at which a droplet traverses an electrode pitch length ($e = 1.56$ mm) during a single transfer[33] (Fig. 5c). Thus, *f* can be represented as $f = \frac{u_{avg}}{e}$. The transfer frequency depends on the average velocity of the droplet, which in turn depends on the applied voltage. There is a 15% overall improvement in transfer frequency over the entire voltage range 200V – 350V. The value of *f* is indicative of the transport performance of the fabricated DMF platform.

Figure 6 is a comparison of the experimentally measured values of u_{avg} and that predicted fro[illegible]tion (13). The values of μ_f and ζ are taken to be 8.9×10^{-4} Pa.s and 0.046 Pa.s respectively. The values of ζ are obtained by comparing the theoretical (equation 13) and the experimental average velocities and are comparable to the reported values in the literature (0.04-0.08 Pa.s in [31]) highlighting the efficacy of equation (13) for explaining droplet transport on a DMF platform.

(c)

3.4 Quantitative estimation of droplet transport on triangular and square electrodes

The time taken by a droplet to traverse an effective pitch length (*e*) for a specific *V* is termed as the droplet transfer time (t_{tr}). It is observed that the major difference between the conventional square electrode systems and the fabricated triangular electrodes used in the present study is in the values of t_{tr} for a single transfer. Fig. 7 represents the schematic representation of the top view of a sessile droplet over triangular as well as a square electrode for a single transfer. The length (*L*) and the inter-electrode gap (*p*) for both types of electrodes are kept the same (*L*= 1.5 mm and *p*=60 μm). The effective length traversed by the droplet in a single transfer over triangular activated electrode is defined as, $e = \left(\frac{\sqrt{3}}{2}\cdot L\right) + p$ and that for square electrode can be represented as, $e' = L + p$ respectively. Thus the t_{tr} can

be expressed as, $t_{tr} = \frac{e}{u_{avg}}$ for triangular and $t_{tr}' = \frac{e'}{u_{avg}}$ for the square electrode. Therefore for identical applied voltage, droplet volume, dielectric material, and thickness, t_{tr} should approximately scale with e (or e'). As the effective pitch length for triangular electrodes is less than the square electrode the estimated increase in a transfer rate over the triangular electrode is about 15%.

The average velocities (u_{avg}) obtained from the experimental data for triangular electrodes are further compared with those from another similar study employing conventional square electrodes[34]. It needs to be pointed out that in that study PDMS was used as the dielectric-hydrophobic layer having a thickness of 15μm and inter-electrode gap of 80μm. Thus the comparison will only provide a qualitative indication of the increase in transfer efficiency for the present case. The comparison shows appreciable overall improvements in u_{avg} for all the applied voltages (Fig. 8).

4. CONCLUSION

The unique design of the fabricated triangular electrodes on the DMF platform resulted in a zigzag motion of the droplet due to the continuous changing of the direction of the net motive force on the contact line. Significant reductions in transfer time (about 15%) for droplet movement along with improvement in average droplet velocities on the fabricated DMF platform are observed, quantified and compared to results on conventional square electrodes. A model based on a force balance approach between the driving and the resistive forces is developed and the resulting equations are used to analyze the experimental trends and results. The droplet spreading dynamics is thoroughly probed and the values of the ratio of the characteristic time scales (ξ) at the underdamped and overdamped regimes are evaluated. The values of ξ for the present experimental system and applied voltage range

indicate that the droplet dynamics follows the characteristics of an underdamped regime. The values of the contact line friction coefficient are evaluated from the experimental data and are found to be consistent with the values reported in the literature. These results will be helpful in developing micro-actuators with a faster response in lab-on-chip applications.

ACKNOWLEDGEMENT

The authors gratefully acknowledge the financial support provided by Indian Space Research Organization (ISRO) through the Kalpana Chawla Space Technology Cell, Indian Institute of Technology Kharagpur, India [Sanction Letter No: IIT/KCSTC/Chair./NEW/P/17-18/01, Dt. 17-05-2017] and the support of Dr. Amrit Ambirajan and and Dr. V. S. Jasvanth of the Thermal Systems Group, ISRO Satellite Centre, Bangalore, India.

REFERENCES

[1] V. Srinivasan, V. K. Pamula, and R. B. Fair, "An integrated digital microfluidic lab-on-a-chip for clinical diagnostics on human physiological fluids. *Lab on a chip*, 4(310-315), 2004.

[2] Y. Li, R. J. Baker, and D. Raad, "A Highly Efficient and Reliable Electrowetting on Dielectric Device for Point-of-Care Diagnostics," in *IEEE Dallas Circuits and Systems Conference (DCAS)*, 2015.

[3] T. Lin, D. Yao, T. Lin, and D. Yao, "Applications of EWOD Systems for DNA Reaction and Analysis Applications of EWOD Systems for DNA Reaction and Analysis," vol. 4243, no. May, 2012.

[4] W. Wang, J. Chen, and J. Zhou, "Droplet generating with accurate volume for EWOD digital microfluidics," *Proc. - 2015 IEEE 11th Int. Conf. ASIC, ASICON 2015*, vol. m,

pp. 8–11, 2016.

[5] G. Bindiganavale, S. M. You, and H. Moon, “Study of hotspot cooling using electrowetting on dielectric digital microfluidic system,” *Proc. IEEE Int. Conf. Micro Electro Mech. Syst.*, pp. 1039–1042, 2014.

[6] S. Kuiper and B. H. W. Hendriks, “Variable-focus liquid lens for miniature cameras,” *Appl. Phys. Lett.*, vol. 85, no. 7, pp. 1128–1130, 2004.

[7] J. Heikenfeld *et al.*, “Electrofluidic displays using Young-Laplace transposition of brilliant pigment dispersions,” *Nat. Photonics*, vol. 3, no. 5, pp. 292–296, 2009.

[8] Y. H. Chang, G. Bin Lee, F. C. Huang, Y. Y. Chen, and J. L. Lin, “Integrated polymerase chain reaction chips utilizing digital microfluidics,” *Biomed. Microdevices*, vol. 8, no. 3, pp. 215–225, 2006.

[9] M. Abdelgawad, S. L. S. Freire, H. Yang, and A. R. Wheeler, “All-terrain droplet actuation,” *Lab Chip*, vol. 8, no. 5, p. 672, 2008.

[10] S. K. Cho, H. Moon, and C. Kim, “Creating , Transporting , Cutting , and Merging Liquid Droplets by Electrowetting-Based Actuation for Digital Microfluidic Circuits,” vol. 12, no. 1, pp. 70–80, 2003.

[11] C. G. Cooney, C. Y. Chen, M. R. Emerling, A. Nadim, and J. D. Sterling, “Electrowetting droplet microfluidics on a single planar surface,” *Microfluid. Nanofluidics*, vol. 2, no. 5, pp. 435–446, 2006.

[12] J. Berthier, *Microdrops and digital microfluidics.* 2008.

[13] S. Chakraborty and R. Mittal, “Droplet dynamics in a microchannel subjected to electrocapillary actuation Droplet dynamics in a microchannel subjected to

electrocapillary actuation," *J. Appl. Phys.*, vol. 104901, no. 101, pp. 104901–1 to 104901–8, 2007.

[14] J. Berthier, P. Dubois, P. Clementz, P. Claustre, C. Peponnet, and Y. Fouillet, "Actuation potentials and capillary forces in electrowetting based microsystems," *Sensors Actuators A. Phys.*, vol. 134, no. 2, pp. 471–479, 2007.

[15] U. C. Yi and C. J. Kim, "Characterization of electrowetting actuation on addressable single-side coplanar electrodes," *J. Micromechanics Microengineering*, vol. 16, no. 10, pp. 2053–2059, 2006.

[16] L. S. Jang, C. Y. Hsu, and C. H. Chen, "Effect of electrode geometry on performance of EWOD device driven by battery-based system," *Biomed. Microdevices*, vol. 11, no. 5, pp. 1029–1036, 2009.

[17] D. Das, S. Das, and K. Biswas, "Effect of Electrode Geometry on Voltage Reduction in EWOD Based Devices," in *2010 International Conference on Systems in Medicine and Biology*, 2010, no. December, pp. 371–375.

[18] X. Xu, L. Sun, L. Chen, Z. Zhou, and J. Xiao, "Electrowetting on dielectric device with crescent electrodes for reliable and low-voltage droplet manipulation," *Biomicrofluidics*, vol. 064107, no. 2014, p. 064107, 2015.

[19] H. Geng, J. Feng, L. M. Stabryla, and S. K. Cho, "Dielectrowetting manipulation for digital microfluidics: creating, transporting, splitting, and merging of droplets," *Lab Chip*, vol. 17, no. 6, pp. 1060–1068, 2017.

[20] Q. Vo, H. Su, and T. Tran, "Universal Transient Dynamics of Electrowetting Droplets," *Sci. Rep.*, pp. 1–7, 2018.

[21] T. D. Blake and J. M. Haynes, “Kinetics of liquidliquid displacement,” *J. Colloid Interface Sci.*, vol. 30, no. 3, pp. 421–423, 1969.

[22] A. L. Biance, C. Clanet, and D. Quéré, “First steps in the spreading of a liquid droplet,” *Phys. Rev. E - Stat. Physics, Plasmas, Fluids, Relat. Interdiscip. Top.*, vol. 69, no. 1, p. 4, 2004.

[23] B. B. CatherineQuilliet, “Electrowetting: a recent outbreak,” *Curr. Opin. Colloid Interface Sci.*, vol. 6, no. 1, pp. 34–39, 2001.

[24] J. Berthier, P. Dubois, P. Clementz, P. Claustre, C. Peponnet, and Y. Fouillet, “Actuation potentials and capillary forces in electrowetting based microsystems,” vol. 134, pp. 471–479, 2007.

[25] A. Ahmadi, H. Najjaran, J. F. Holzman, and M. Hoorfar, “Two-dimensional flow dynamics in digital microfluidic systems,” *J. Micromechanics Microengineering*, vol. 19, no. 6, p. 065003, 2009.

[26] H. Ren, R. B. Fair, M. G. Pollack, and E. J. Shaughnessy, “Dynamics of electro-wetting droplet transport,” *Sensors Actuators, B Chem.*, vol. 87, no. 1, pp. 201–206, 2002.

[27] R. Dey, U. U. Ghosh, S. Chakraborty, and S. DasGupta, “Dynamics of Electrically Modulated Colloidal Droplet Transport,” *Langmuir*, vol. 31, no. 41, pp. 11269–11278, 2015.

[28] S. Datta, A. K. Das, and P. K. Das, “Unravelling Electrostatic Actuation on Inclined and Humped Surfaces: Effect of Substrate Contact Angle,” *Ind. Eng. Chem. Res.*, vol. 55, no. 14, pp. 3949–3959, 2016.

[29] M. J. De Ruijter, M. Charlot, M. Voué, and J. De Coninck, “Experimental evidence of several time scales in drop spreading,” *Langmuir*, vol. 16, no. 5, pp. 2363–2368, 2000.

[30] D. Seveno, A. Vaillant, R. Rioboo, H. Adão, J. Conti, and J. De Coninck, “Dynamics of wetting revisited,” *Langmuir*, vol. 25, no. 22, pp. 13034–13044, 2009.

[31] T. D. Blake, “The physics of moving wetting lines,” *J. Colloid Interface Sci.*, vol. 299, no. 1, pp. 1–13, 2006.

[32] W. C. Nelson and C. C. J. Kim, “Journal of Adhesion Science and Droplet Actuation by (EWOD): A Review,” *J. Adhes. Sci. Technol.*, vol. 26, no. August 2012, pp. 1747–1771, 2012.

[33] D. Son *et al.*, “Experimental test of scaling of mixing by chaotic advection in droplets moving through microfluidic channels,” *Appl. Phys. Lett.*, vol. 86, no. 3, pp. 573–579, 2007.

[34] V. Jain, V. Devarasetty, and R. Patrikar, “Effect of electrode geometry on droplet velocity in open EWOD based device for digital micro fl uidics applications,” *J. Electrostat.*, vol. 87, pp. 11–18, 2017.

TABLE FOR MANUSCRIPT

Augmented Droplet Actuation and Spreading using Triangular Coplanar Electrodes

Table 1: The variation in the values of ξ with the electrowetting number, η.

η	ξ
0.665	0.1807
1.039	0.1733
1.497	0.1638
2.037	0.1627

FIGURES FOR THE MANUSCRIPT

Augmented Droplet Actuation and Spreading using Triangular Coplanar Electrodes

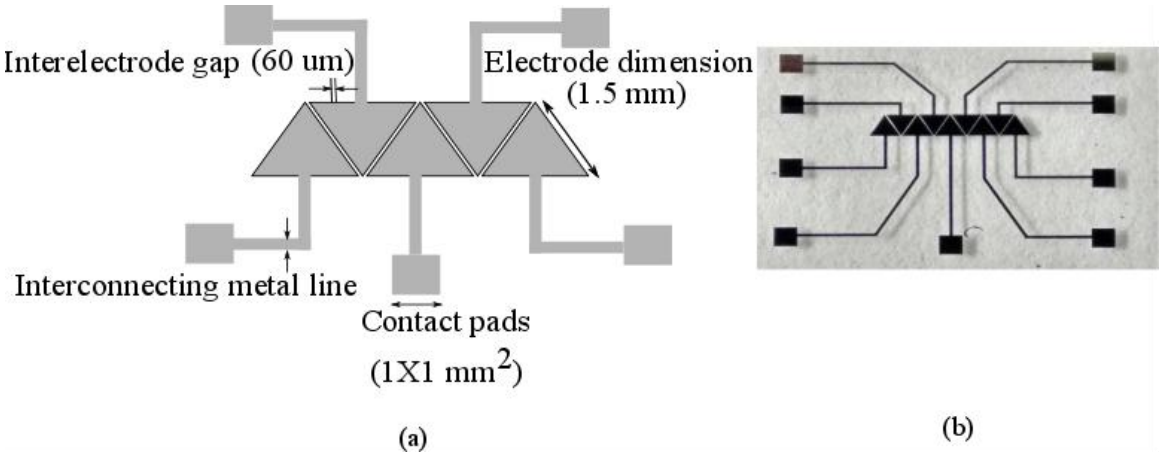

Figure 1: (a) Schematic view of the designed triangular electrode array with the individual contact pads and (b) optical photograph of the fabricated electrode array photomask.

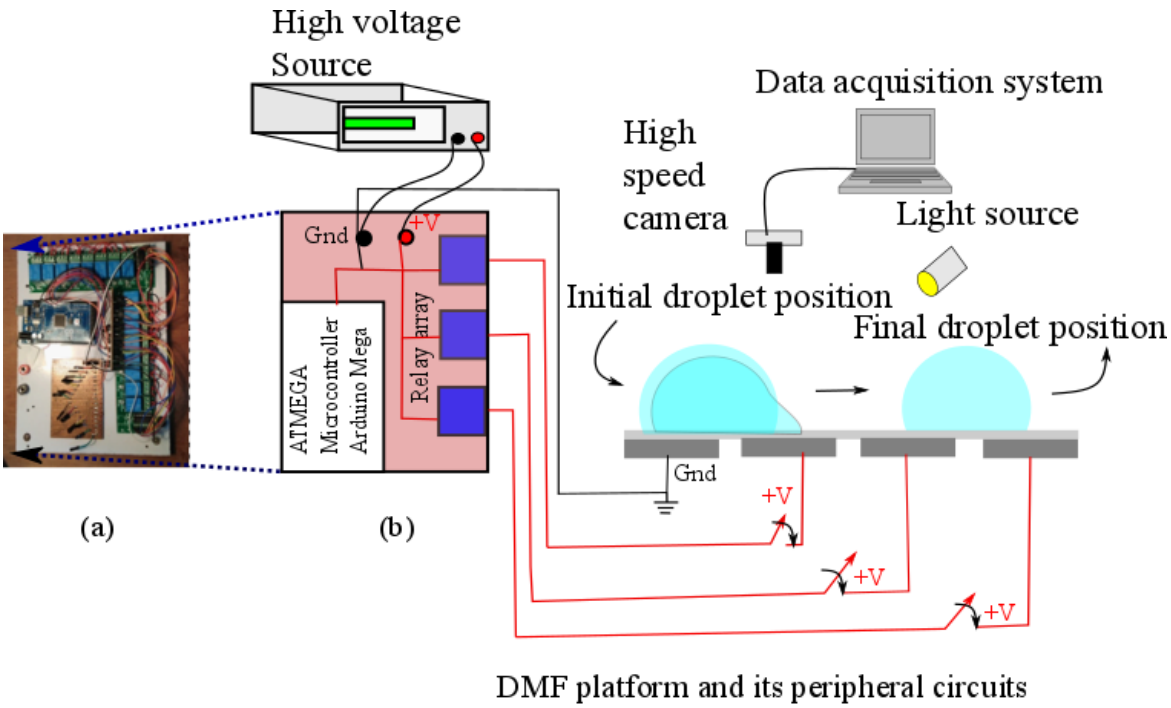

Figure 2: Experimental setup for microdroplet actuation; (a) the Arduino based switching logic circuit, (b) schematic of the setup.

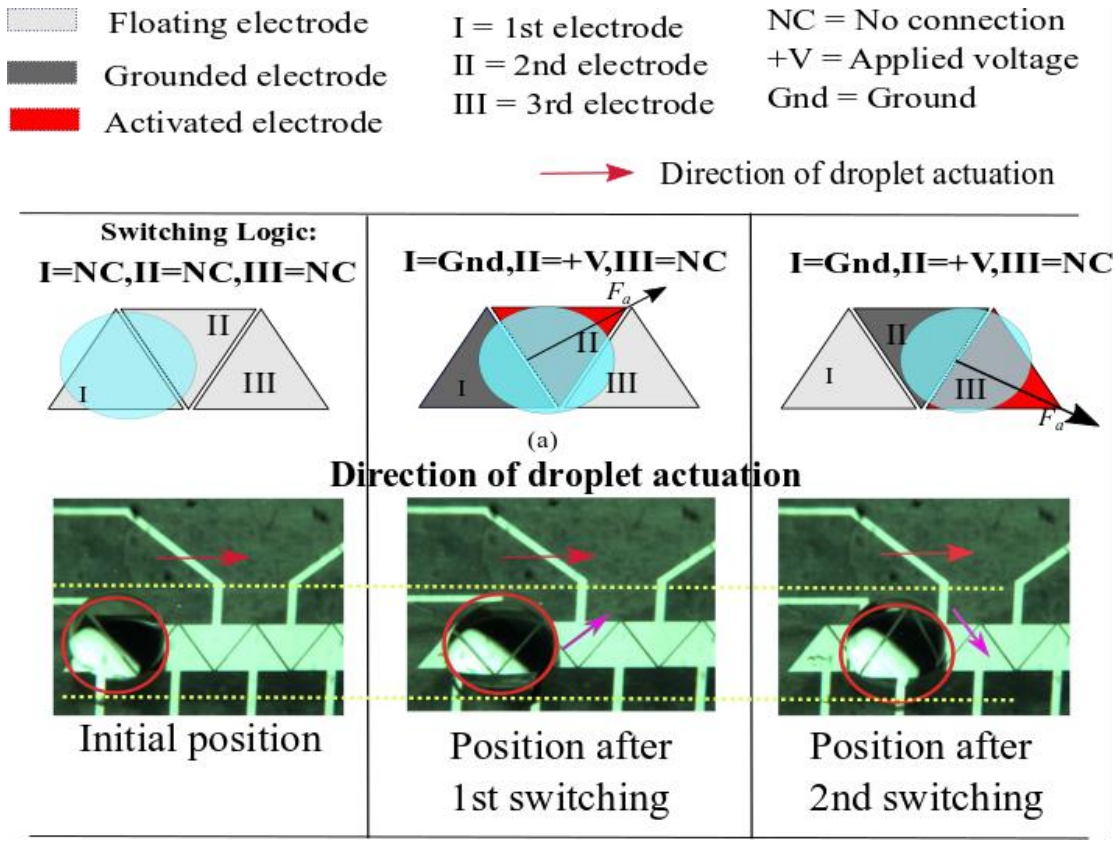

Figure 3: (a) Schematic and (b) photograph of droplet position at three different switching logics during movement; (i) initial droplet position, (ii) position after 1st switching, (iii) position after 2nd switching. F_a represents the driving force.

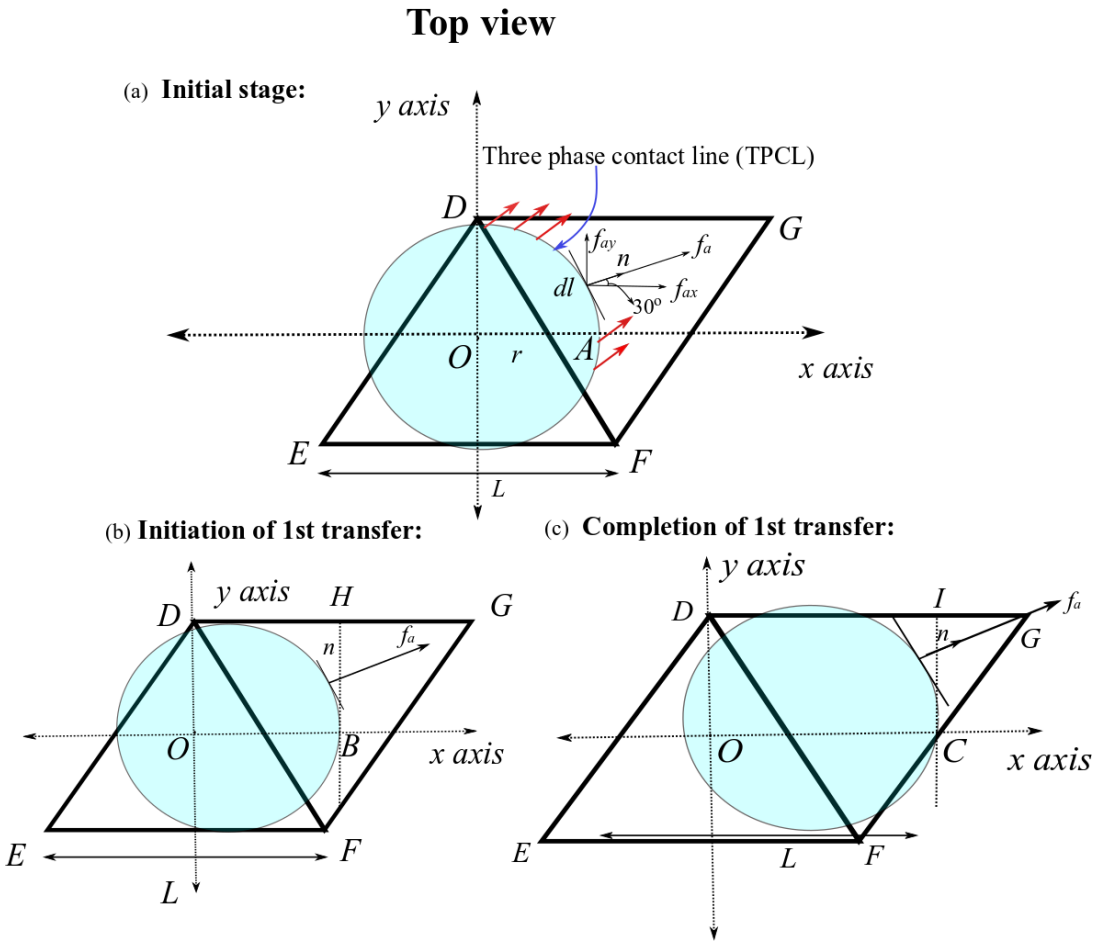

Figure 4: Schematic of the electro-capillary force on the droplet and position of the droplet during 1st transfer; (a) the initial droplet position (red arrow represents the direction of the driving force) (b) position during initiation of 1st transfer and (c) position after the 1st transfer. Positions A, B, and C represent the locations of the advancing region of the droplet over the activated electrodes.

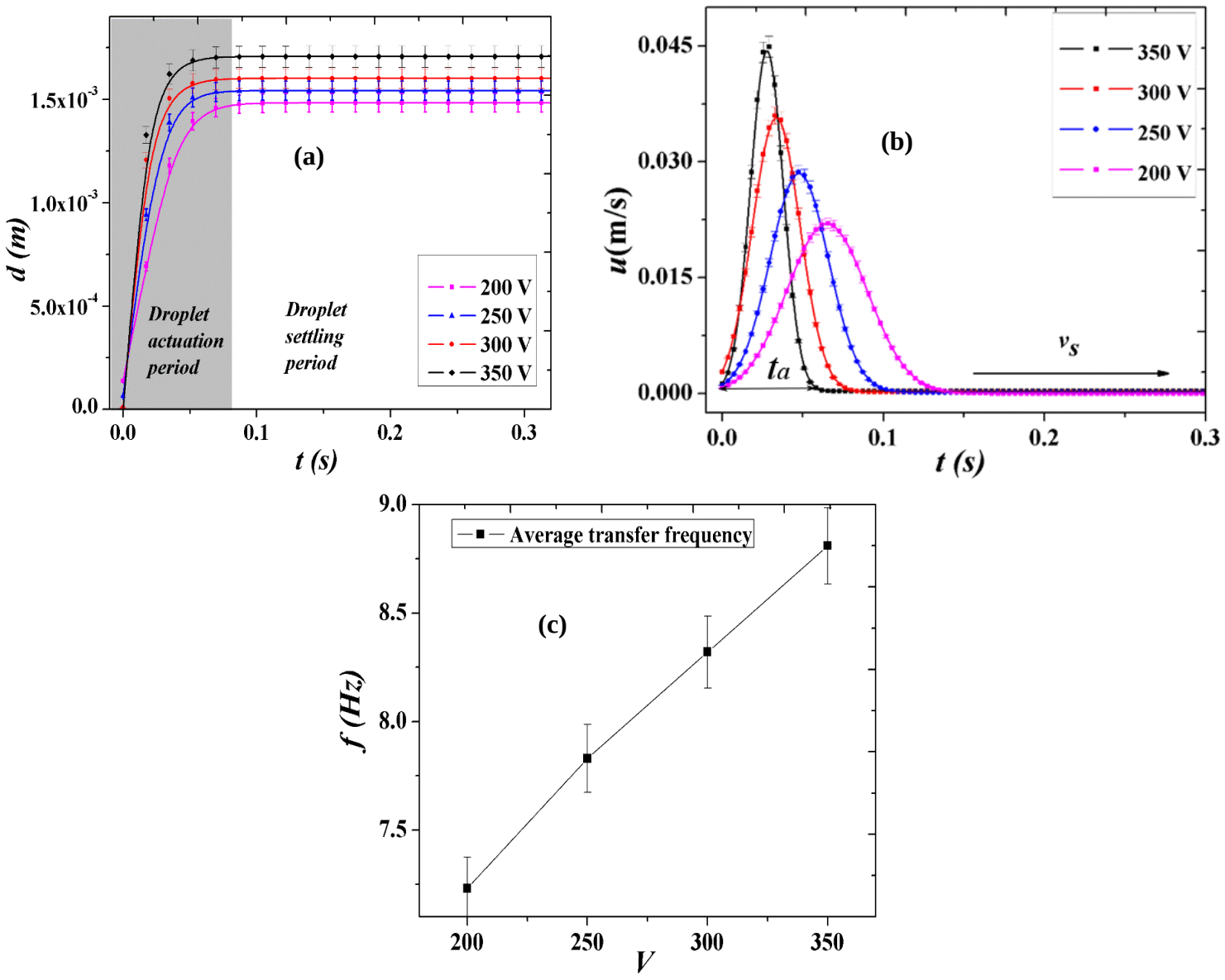

Figure 5: (a) the displacement of the droplet at applied voltages of 200V, 250V, 300V and 350V; (b) corresponding instantaneous velocities after first transport (the lines are the best-fitted curves for the data points); (c) the average transfer frequency at different operating voltages (±1-4% error is associated with each experimental value). The line is a guide for the readers' eyes.

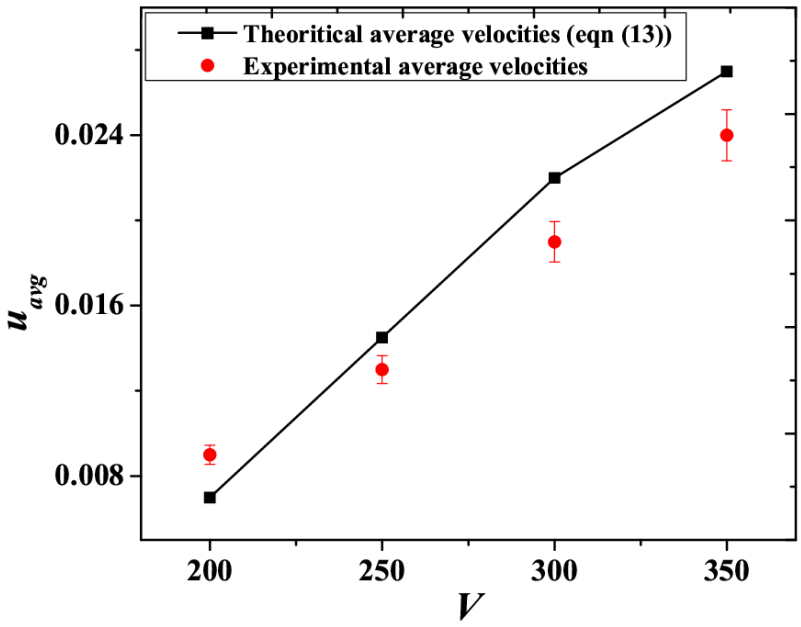

Figure 6: Comparison of the predicted and experimental (±1-4% error) velocities at different applied voltages. The line is a guide for the readers' eyes only.

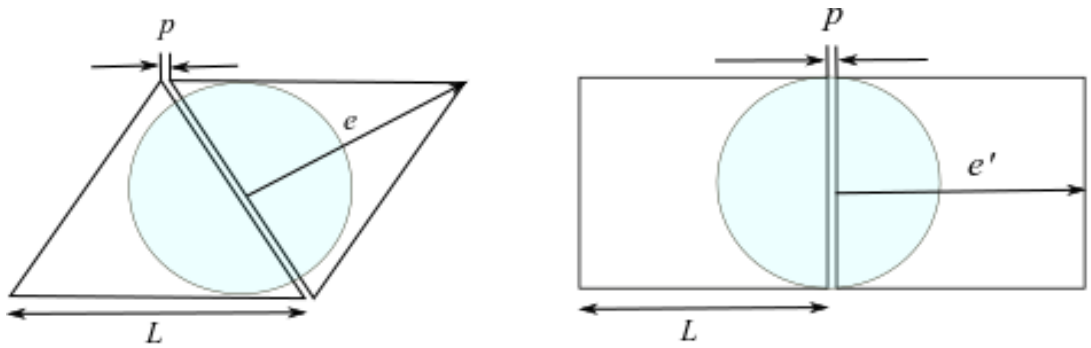

(a) (b)

Figure 7: Comparison of the distance covered by the droplet over (a) triangular and (b) square coplanar electrode array in a single transfer.

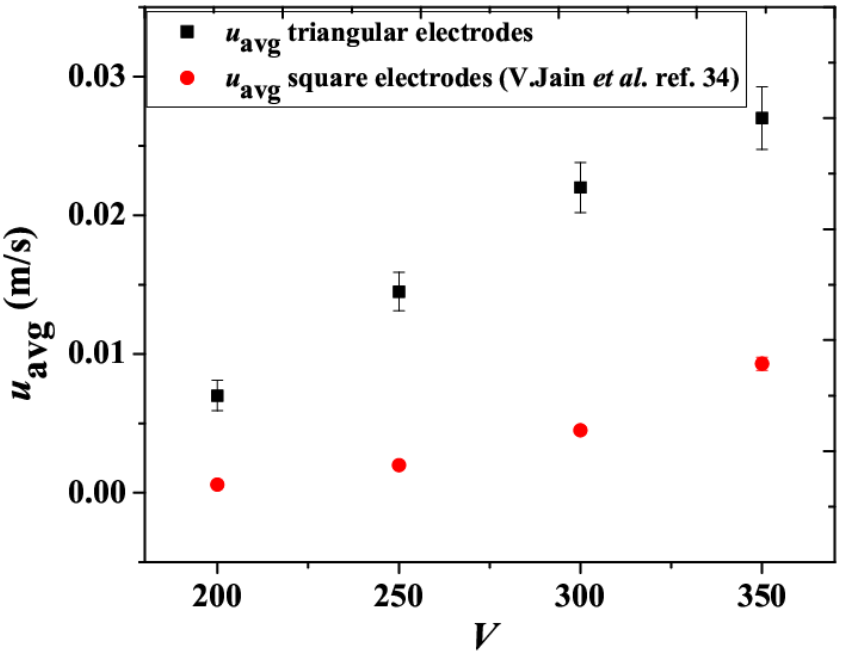

Figure 8: Comparison of the average velocities for the fabricated triangular and conventional square electrodes in DMF platform.

Supplementary Material

Click here to download Supplementary Material: Supplementary documents_manuscript.docx

ABOUT THE AUTHOR(S)

Mainak Basu is working for his PhD at the Advanced Technology Development Centre (ATDC), Indian Institute of Technology Kharagpur with a research interest in micro-droplet actuation using electrowetting on dielectric (EWOD) for digital microfluidic (DMF) applications.

Vedant Pradeep Joshi is an undergraduate student of the Chemical Engineering Department at Indian Institute of Technology Kharagpur.

Dr. Soumen Das is a Professor of the School of Medical Science and Technology, Indian Institute of Technology Kharagpur. His research area includes Bio-MEMS and microsystems, sensors and actuators, biomedical devices and flexible electronics.

Dr. Sunando DasGupta is a Professor of the Department of Chemical Engineering and Head of the Advanced Technology Development Centre (ATDC), Indian Institute of Technology Kharagpur. His research area includes microfluidics, micro-scale transport process, droplet dynamics and interfacial phenomena.

Multimedia: Audio/Video

Click here to download Multimedia: Audio/Video: Droplet actuation video.avi